Title	Characterization, Modeling and Analysis of Organic Light-Emitting Diodes With Different Structures
Author(s)	Chen, H; Choy, WCH; Hui, SYR
Citation	IEEE Transactions on Power Electronics, 2015
Issued Date	2015
URL	http://hdl.handle.net/10722/210728
Rights	Creative Commons: Attribution 3.0 Hong Kong License

This article has been accepted for publication in a future issue of this journal, but has not been fully edited. Content may change prior to final publication. Citation information: DOI 10.1109/TPEL.2015.2403618, IEEE Transactions on Power Electronics

Characterization, Modeling and Analysis of Organic Light-Emitting Diodes With Different Structures

H.T. Chen[1], Wallace C.H. Choy[1] , Senior *Member, IEEE* and S.Y.R. Hui[1,2], *Fellow, IEEE*

1 Department of Electrical & Electronic Engineering, The University of Hong Kong, Pokfulam Road, Hong Kong.

2 Department of Electrical & Electronic Engineering, Imperial College London

Abstract: This paper demonstrates that organic light-emitting diodes (OLEDs) of different structures can be characterized and modeled using a combination of the photo-electro-thermal (PET) theory and spectral power distribution modeling. The photometric, electrical, thermal and chromatic properties of OLED devices are incorporated into a model framework so that the performance of OLED of different structures can be compared. A concept of luminance uniformity over the OLED surfaces is also introduced for comparing OLED with large surface areas. Experimental results are included to verify the OLED models and compare the characteristics of two different OLED samples. Based on the same PET framework, some differences of OLEDs and inorganic LEDs are addressed and discussed.

Keywords: Organic light-emitting diodes (OLED), Lighting systems, Photo-Electro-Thermal (PET) theory

I. INTRODUCTION

Recent progress in organic light-emitting diodes (OLEDs) have attracted considerable attention because they have wide viewing angle, fast response and the potential of being mechanically thin

This article has been accepted for publication in a future issue of this journal, but has not been fully edited. Content may change prior to final publication. Citation information: DOI 10.1109/TPEL.2015.2403618, IEEE Transactions on Power Electronics

and flexible [1],[2]. Since the report of first low voltage OLED using a simple bi-layer structure [3], intensive studies have been conducted from organic materials to device structures. Meanwhile, in 1998, phosphorescent OLEDs were demonstrated in which the emissive materials were osmium complexes doped in poly(9-vinylbarbazole) (PVK)[4]. In the same year, the use of platinum porphyrin doped in *tris* (8-hydroxyquinoline) aluminum (Alq_3) host as the phosphorescence light emitters was also reported [5]. Since then, a platform has also been developed for the use of phosphorescent light emitting based metal complexes in OLED technology [6]. Phosphorescent emitters to quadruple the device efficiency have been demonstrated by harvesting both singlet and triplet excitation through efficient intersystem crossing enabled by the presence of heavy metal in the emitter [5]. The efficiency of organic electroluminescent devices could be further improved by cohosting the electron dominant complex such as into the typical electron transporting layer [7]. Meanwhile, other approaches such as doping fluorescent- and phosphorescent- type emitters individually into two different hosts separated by an interlayer to form a fluorescence-interlayer-phosphorescence emission to enhance the efficiency of OLEDs were developed [8].

Currently, there are a range of OLED structures for white light generation. The first white OLED was demonstrated by color mixing [9]. One simple approach is to co-deposit three phosphorescent emitters into a single host to form a single emissive layer [10]. Another approach is to use a fluorescent blue emitter together with phosphorescent green and red emitters to construct a three color white device [11]. The blue phosphorescent OLEDs generally have short lifetimes and large roll-off issues as compared to their fluorescent counterparts [12]. Nevertheless, blue phosphorescent OLEDs are still attractive due to its high luminous efficacy and various approaches have been proposed to improve the efficiency and color quality [8],[13]. Tandem white OLEDs,

This article has been accepted for publication in a future issue of this journal, but has not been fully edited. Content may change prior to final publication. Citation information: DOI 10.1109/TPEL.2015.2403618, IEEE Transactions on Power Electronics

which comprise vertically stacked layers electrically interconnected by a compound MoO_3/Li-doped charge generation layer are reported in [11]. White OLEDs of the multiple emissive layers such as separate emissive layers [14] and cascade emissive layers [15] have also been studied. Recently, the single emitter white OLED also has considerable progress and the peak power efficiency reaches 56.7lm/W [16]. Efficiency of such white OLED structure can be improved by combining a chosen emitter layer with high-refractive-index substrates, and using a periodic out-coupling structure [17].

Although white OLEDs have already out-performed incandescent lights and halogen lamps in efficacy, currently their performance is still far from the target of general illumination in terms of high efficiency, long lifetime, light quality, and low cost. Variation of temperatures leads to non-uniform depreciation of its light output, which in turn increases the luminance non-uniformity over time and affects the lifetime of OLED. The optical measurement technique for determination of the spatial temperature distribution at organic layer lever in OLED is proposed [18]. By modeling electro-thermal interaction within OLEDs and precisely describing local heat generation in all electrically active layers of OLEDs accurate prediction of OLEDs' operational characteristics can be obtained [19]. The luminous efficacy of OLED still lags behind the performance of white LED. However, with the future improvements in OLED performance favorably predicted, major lighting companies are actively exploring the energy-saving potential of organic solid-state lighting for general illumination [20].

Despite the wide variety of OLED structures, this paper shows that the frameworks of the PET theory and spectral power distribution modeling can describe the photometric, electric, thermal and chromatic aspects of an OLED system. The OLED model based on such frameworks can be used as a design tool for system evaluation and optimization [21],[22]. Two OLED samples with different structures are used to illustrate the proposed device characterization and modeling principle. Tests

This article has been accepted for publication in a future issue of this journal, but has not been fully edited. Content may change prior to final publication. Citation information: DOI 10.1109/TPEL.2015.2403618, IEEE Transactions on Power Electronics

have been conducted to extract their model parameters such as coefficient k_e (coefficient of the temperature-dependent luminous efficacy), coefficient k_h (heat dissipation coefficient), thermal resistance R_{th}, and spectral characteristics. These parameters are then used for performance analysis and comparative study on the two different OLED structures.

II. CHARACTERIZATION AND PET MODELING OF OLED

Two OLED devices from two manufacturers (Lumiotec and Osram), as shown in Fig 1, are used in this study for device characterization and modeling. The OLED samples are (a) Lumiotec model number: Lumiotec LTS-10015 [23]) and (b) Osram model number: Osram Orbeos CMW-031 [24]. These two OLED devices have two different structures. Their structural difference will be revealed progressively in the device characterization and modeling process. For both OLED samples, the organic layers have to be protected against air as they are sensitive to moisture and oxygen. A substrate is glued onto the back of each OLED in order to enhance the stability of the permeation barrier and thermal conduction. Optical measurements of the OLED samples are conducted under steady-state thermal and electrical conditions using a PMS-50 spectro-photocolorimeter with an integrating sphere. The steady-state measurements are obtained after 20 minutes of operation at respective electrical power levels at an ambient temperature of 20^{o}C. The voltage changes of the devices during the process of heating can be captured by using Transient Thermal Tester (T3ster) based on thermal transient measurement procedure. Besides the combined thermal and optical measurement, the temperature dependence of optical power and the wall-plug efficiency of the OLED are also measured and recorded based on the use of the TeraLED system. The schematic of the experimental setup is shown in Fig 2. The theoretical framework of evaluation of T3Ster is based on the distribution RC networks [25].

This article has been accepted for publication in a future issue of this journal, but has not been fully edited. Content may change prior to final publication. Citation information: DOI 10.1109/TPEL.2015.2403618, IEEE Transactions on Power Electronics

The T3ster captures the thermal transient response in real time, records the cooling/heating curve and then evaluates the cooling/heating curve in order to obtain the thermal characteristics. For voltage-temperature sensitivity calibration, a 0.005 A current is applied in a temperature-controlled oven (at different ambient temperature of 25 ^{o}C, 40 ^{o}C, 55 ^{o}C and 70 ^{o}C) under pulsed-current injection with small duty cycle by using Keithley 2400 SourceMeter. Then the junction temperature is obtained in each case from the OLED through the use of the voltage response curve and voltage-temperature sensitivity calibration using the T3Ster system. The luminance and temperature distribution of the samples at different current levels are captured by LUMICAM 1300 imaging photometer/colorimeter and LWIR camera (FLIR SC645).

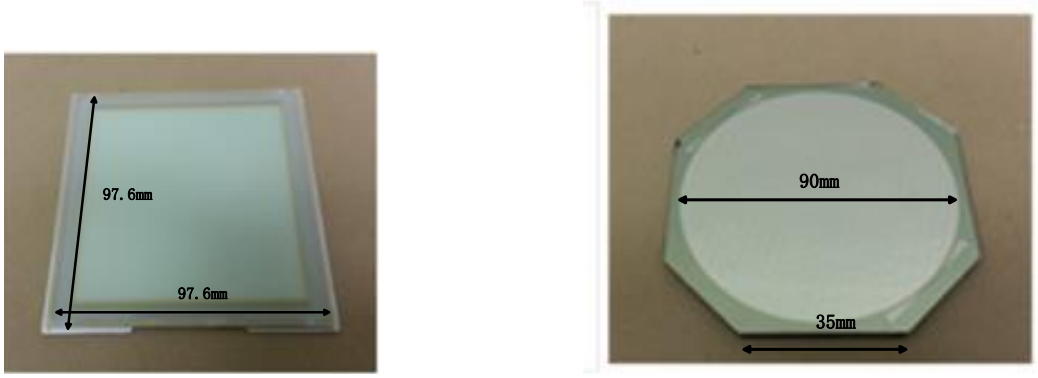

(a) (b)

Fig. 1 Simplified device structures for OLED(a) Lumiotec LTS-10015 (b) Osram Orbeos CMW-031

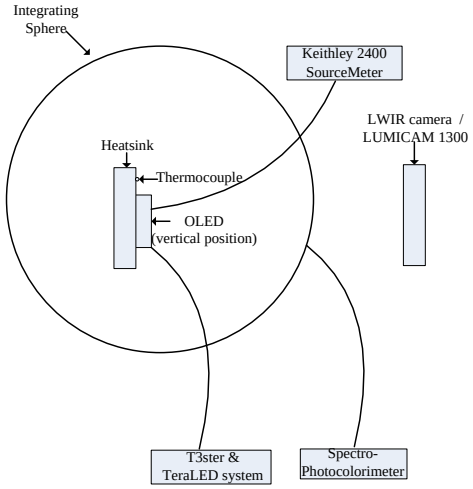

Fig.2 Schematic of the experimental setup

This article has been accepted for publication in a future issue of this journal, but has not been fully edited. Content may change prior to final publication. Citation information: DOI 10.1109/TPEL.2015.2403618, IEEE Transactions on Power Electronics

III. IMPORTANT CHARACTERISTICS OF OLED

A. Rate of Reduction of Luminous Efficacy with Junction Temperature k_e

The luminous intensity I of lighting devices is an expression of the amount of light power emitting from light source within a solid angle, which is a function of the junction temperature. At near room temperature, the emission intensity follows an exponential decay function [26].

$$I = I\big|_{25^oC} \exp\frac{-(T_j - 25^oC)}{T_1} \tag{1}$$

where T_1 is the characteristic temperature of the device and T_j is the junction temperature. A high characteristic temperature implies that the luminous flux is weakly dependent on junction temperature, which is a desirable feature and can be used as an indicator for comparing the OLED samples. The luminous intensity could be derived from the expression of luminous efficacy E, which is given by

$$E = E\big|_{25^oC} \exp\left(-\frac{T_j - 25^oC}{T_1}\right) \tag{2}$$

The luminous flux ϕ_v can be expressed as a function of electrical power P_d.

$$\phi_v = P_d E \tag{3}$$

Fig. 3(a) and (b) show the measured luminous efficacy of the Lumiotec and Osram samples, respectively. The luminous flux of the two samples decreases with increasing junction temperature at different rates. By fitting the measured curve into the form of (2), the characteristic temperature T_1 of the Lumiotec and Osram samples are 1416 ^{o}C and 512 ^{o}C, respectively. This suggests that the luminous efficacy of the Lumiotec sample decreases at a slower rate with increasing junction temperature than that of the Osram sample.

This article has been accepted for publication in a future issue of this journal, but has not been fully edited. Content may change prior to final publication. Citation information: DOI 10.1109/TPEL.2015.2403618, IEEE Transactions on Power Electronics

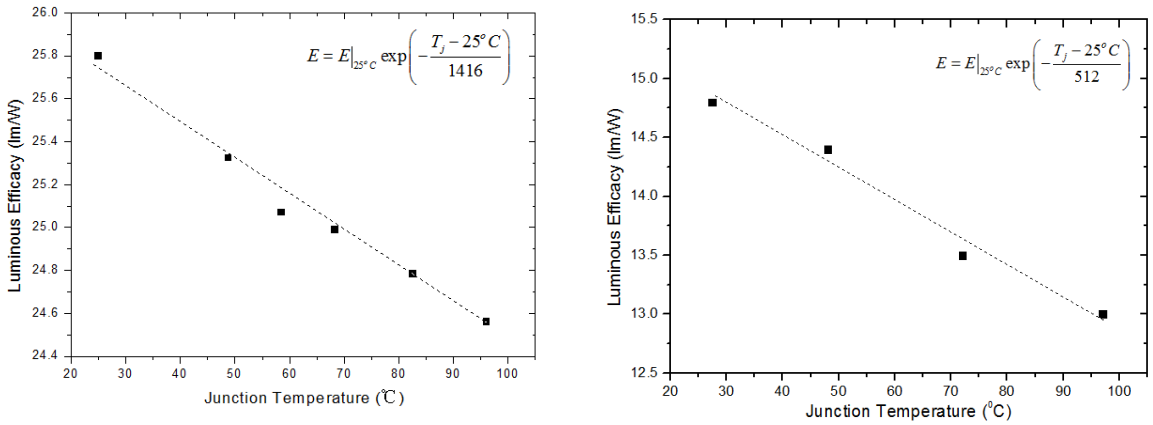

(a) (b)

Fig. 3 Measured luminous efficacy versus junction temperature (a) Lumiotec LTS-10015 (b) Osram Orbeos CMW-031

The coefficient k_e defined in the PET theory [21],[22] is a measure of the droop characteristic of the luminous efficacy with junction temperature and is physically related to the characteristic temperature [27]:

$$k_e = -\frac{1}{T_1} \tag{4}$$

The coefficient k_e can therefore be determined from the characteristic temperature of the device, where k_e for Lumiotec OLED sample is about -0.00071 $^{o}C^{-1}$ and that for Osram OLED sample is about -0.0019 $^{o}C^{-1}$. The Lumiotec sample is less sensitive to temperature change than the Osram sample. When projected to 25 ^{o}C, the luminous efficacy E_o of the Lumiotec and Osram samples are 25.8 and 14.8lm/W, respectively.

Remarks:

It is interesting to compare typical characteristics of OLEDs and inorganic LEDs. The two inorganic white LED samples characterized with the PET theory are used for comparison as shown

This article has been accepted for publication in a future issue of this journal, but has not been fully edited. Content may change prior to final publication. Citation information: DOI 10.1109/TPEL.2015.2403618, IEEE Transactions on Power Electronics

in Table I. It can be seen that the OLED devices generally have lower luminous efficacy than inorganic LED ones. But with a larger surface area, it is possible to design OLED with a very small k_e, indicating that the droop characteristics of OLED with temperature can be designed to be much smaller than those of inorganic LEDs. This means that OLED can be less sensitive with temperature changes.

Table I Comparison of luminous efficacy and droop rate of OLEDs and inorganic LEDs

	Organic LED *Lumiotec LTS-10015*	Organic LED *Osram Orbeos CMW-031*	Inorganic LED *Sharp GW5BWF15L00*	Inorganic LED *Cree XREWHT-L1-0000-00C01*
E_o *(lm/W)*	25.8	14.8	96.0	87.0
k_e ($^oC^{-1}$)	-0.00071	-0.0019	-0.0039	-0.0023

*B. **Heat dissipation Coefficient k_h***

Theoretically, the input electrical power of lighting devices will not be transformed completely into photon energy. There is heat generated within the chip due to non-radiative, auger recombination *etc* [28],[29]. Therefore, the output energy transformed from electrical power can be divided into optical power and heat dissipation power. The heat dissipation coefficient k_h [27] represents the portion of LED power that is dissipated as heat. It is related to the optical power and wall-plug efficiency η_w that can be measured by combined thermal and radiometric measurement equipment. Therefore, k_h is a factor that can be used for comparing heat dissipation of the samples. The goal of this section is to study the variation of heat dissipation for lighting devices with different electrical power.

This article has been accepted for publication in a future issue of this journal, but has not been fully edited. Content may change prior to final publication. Citation information: DOI 10.1109/TPEL.2015.2403618, IEEE Transactions on Power Electronics

According to the previous reports about LED device, within the practical ranges of the operating temperature (maximum allowance junction temperature: 125 ^{0}C) and electrical power (dependent on heatsink size and rated power), the reduction of wall-plug efficiency with increasing junction temperature is fairly linear and the reduction of wall-plug efficiency with increasing electrical power is fairly parabolic. It has been mathematically proved [30] that k_h is a two-dimensional function of electrical power and temperature. It can be approximated as:

$$\begin{aligned} k_h &= 1-\frac{P_{opt}}{P_d} = 1-\eta_w \\ &= 1-\frac{(\sigma T_{hs}+\tau)(\chi P_d^{\,2}+\delta P_d+\gamma)}{\mu} \end{aligned} \tag{5}$$

where P_{opt} is optical power, T_{hs} is heatsink temperature, P_d is electrical power, η_w is wall-plug efficiency, σ, τ ,χ, δ, γ, μ are constant coefficients dependent on sensitivity thermal-optical-electrical characteristics of device.

The measured heat dissipation coefficient k_h values for OLEDs are shown in Fig. 4. The OLED samples under test are mounted to a Peltier-based cold-plate with 10 W heat-sinking capability (controlled-temperature heatsink), which is used to stabilize the LED temperature for the optical measurements and serves as a temperature-controlled cold-plate for thermal measurements. The OLED samples are fixed on the controlled-temperature heatsink by a thin layer of thermal adhesive with high thermal conductivity. The thermal resistance of thermal adhesive is ignored in this work. At the controlled heatsink temperature of 24.3 ^{0}C, k_h for Osram LED is about 0.959 under electrical power of 0.3 W. When the electrical power is 4.8 W, k_h increases to 0.978, which indicates the variation k_h with different electrical power is only about 1.9 %. For Lumiotec OLED device, with a heatsink temperature of 22 ^{o}C, k_h for LED is about 0.915 under electrical power of 1W. When the electrical power is 6.5W, k_h only increases to 0.933, which means the variation k_h with different

This article has been accepted for publication in a future issue of this journal, but has not been fully edited. Content may change prior to final publication. Citation information: DOI 10.1109/TPEL.2015.2403618, IEEE Transactions on Power Electronics

electrical power is about 2.1%. This result highlights the important fact that, k_h is fairly constant with increasing operating power. It is noted that the variation of k_h in both samples are kept within very narrow ranges. For the Lumiotec sample, k_h is within 0.906 to 0.937. For the Osram sample, it is within 0.959 to 0.987. In both cases, the amount of OLED power that ends up as heat exceeds 90% of the total OLED power P_d. The Lumiotec sample is more optically efficient than the Osram sample. This is also reflected from their respective E_o values obtained in the previously section.

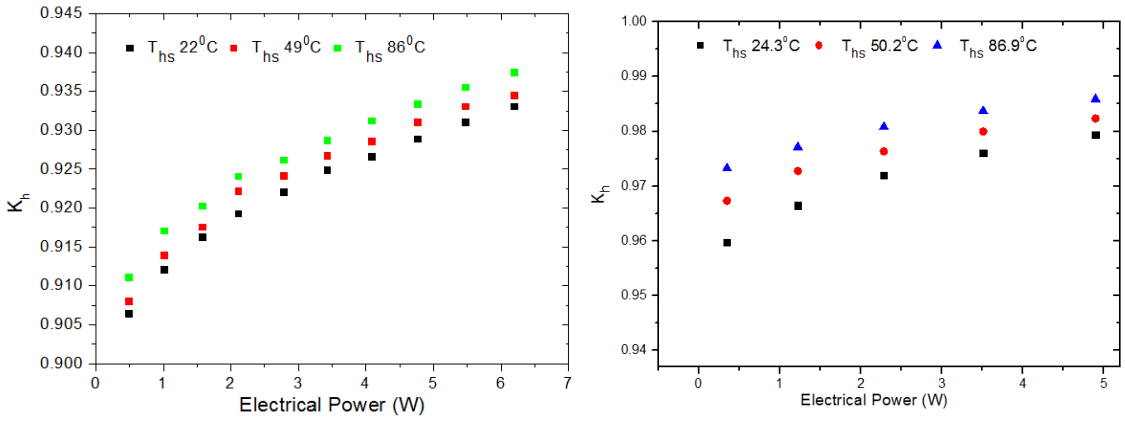

(a) (b)

Fig. 4 Measured heat dissipation coefficient k_h versus electrical power (a) Lumiotec LTS-10015 (b) Osram Orbeos CMW-031

Remark:

Table II shows the heat dissipation coefficients of the same set of organic and inorganic LEDs. Two important observations should be noted. Firstly, the variation ranges of k_h of the OLEDs are much narrower than those of inorganic LEDs. Secondly, the heat dissipation coefficients of OLEDs are generally higher than those of inorganic LEDs. This comparison reflects the state of arts of the two technologies in the current situation. Although OLEDs dissipate a portion of the input power as heat, their large surface areas and contact areas provide better heat transfer than those of the inorganic LEDs which have much smaller surface and contact areas.

This article has been accepted for publication in a future issue of this journal, but has not been fully edited. Content may change prior to final publication. Citation information: DOI 10.1109/TPEL.2015.2403618, IEEE Transactions on Power Electronics

Table II Comparison of heat dissipation coefficients of OLEDs and inorganic LEDs over a typical range of operating power

	Organic LED *Lumiotec LTS-10015*	Organic LED *Osram Orbeos CMW-031*	Inorganic LED *Sharp GW5BWF15L00*	Inorganic LED *Cree XREWHT-L1-0000-00C01*
k_h *(typical)*	0.905 – 0.937	0.959 – 0.987	0.72-0.86	0.67 – 0.84

C. Thermal resistance R_{jc}

Thermal resistance is another key issue for OLED comparison. Similar to the conventional lighting sources such as incandescent lamps, fluorescent lamps and inorganic LEDs, OLEDs generate a significant amount of heat (over 90% of the OLED power as heat). The thermal resistance for convection and radiation is highly dependent on the outer area of the device surface. Unlike inorganic LEDs, OLEDs have much larger surface areas for better?? (higher/ larger?) heat loss through convection and radiation. However, the joule heating problem always exists in the devices. Due to low thermal conductivity of organic materials, there is a need for the use of a substrate to enhance heat transfer of device. The heat transfer property of different substrates is investigated in this study.

For a flat OLED package with a relatively large surface area, the bidirectional heat flow on both sides of the flat OLED package should be considered [31],[[32]. There are two heat dissipation paths: one is downward through the organic layers to the substrate, and the other one is upward through the encapsulant to the packaging surface.

The junction temperature T_j of the device could be accurately captured by T3ster & TeraLED

This article has been accepted for publication in a future issue of this journal, but has not been fully edited. Content may change prior to final publication. Citation information: DOI 10.1109/TPEL.2015.2403618, IEEE Transactions on Power Electronics

systems based on the transient electrical measurements and voltage-temperature characteristics of the device. The difference between the injection electrical power P_d and the emitting optical power P_{opt} is the total heat dissipation P_{heat}, which includes upward and downward heat dissipation. Therefore, the thermal resistance obtained by T3ster is "equivalent" thermal resistance R_{eq}, which can be expressed as $R_{eq}=(T_j-T_a)/(P_d-P_{opt})= (T_j-T_a)/P_{heat}$. This "equivalent" thermal resistance R_{eq} includes the upward thermal resistance R_{up} and downward thermal resistance R_{down}, which can be expressed as $1/R_{eq}=1/ R_{up}+1/ R_{down}$ [33].

For the measured results in Fig.5, a current of 0.005 A and a heating current (0.3 A for Lumiotec OLED and 0.27 A for Osram OLED) are applied to the devices at the ambient temperature of 20 ^{o}C. The light output and transient thermal curve are measured after the OLED has been operated for 20 minutes. The "equivalent" thermal resistance of the package for Lumiotec OLED (from chip to metal substrate) is 0.59 ^{o}C/W, and that for Osram OLED (from chip to glass substrate) is 3.1 ^{o}C/W. Based on thermal structure functions in Fig.5, the thermal bottleneck of the device can be clearly identified. For Lumiotec OLED, the "equivalent" thermal resistance of metal substrate is about 0.34 ^{o}C/W, which is 58% for total device thermal resistance. For Osram device, the "equivalent" thermal resistance of glass substrate is about 2.6 ^{o}C/W, which is 81% for total device thermal resistance. Clearly, a metal substrate is preferred as it has a lower thermal resistance than a glass substrate.

The most critical element in the thermal characteristics of OLED is the substrate, which is shown in thermal structure function. The thermal resistance of this layer should be as low as possible in order to facilitate heat transfer. For a given thermal conductivity of a material, the thermal resistance can be reduced by increasing the contact area or reducing the thickness. In both approaches to reduce the resistance, the mechanical stress of the layer will be proportionally larger,

This article has been accepted for publication in a future issue of this journal, but has not been fully edited. Content may change prior to final publication. Citation information: DOI 10.1109/TPEL.2015.2403618, IEEE Transactions on Power Electronics

which can cause delamination [34]. For OLED device, the contact area of the substrate is obviously larger than that of conventional LED device.

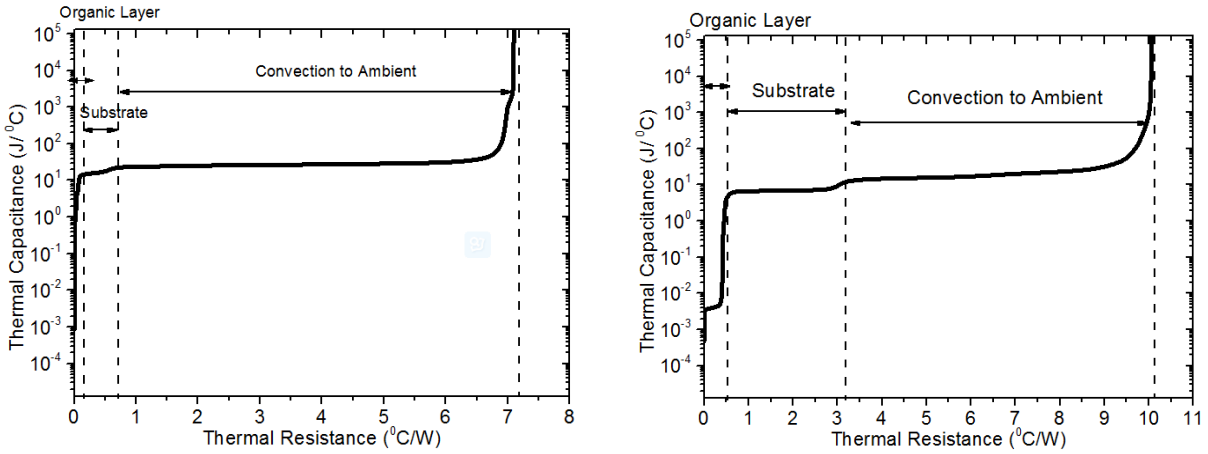

(a) (b)

Fig. 5 Measured thermal structure functions (a) Lumiotec LTS-10015 (b) Osram Orbeos CMW-031

Remark:

Typical thermal resistance of the organic and inorganic LED samples under consideration are tabulated in Table III. The large contact areas give the OLED samples the advantage of having a much lower R_{jc}. The use of metal substrate also enables improved heat transfer and a lower thermal resistance. The results in Table I to Table III suggest that OLEDs are less temperature sensitive than inorganic LEDs.

Table III Comparison of the thermal resistance of OLEDs and inorganic LEDs

	Organic LED *Lumiotec LTS-10015*	Organic LED *Osram Orbeos CMW-031*	Inorganic LED *Sharp GW5BWF15L00*	Inorganic LED *Cree XREWHT-L1-0000-00C01*
R_{jc} (^{o}C/W)	0.59	3.1	6.0	12.0

This article has been accepted for publication in a future issue of this journal, but has not been fully edited. Content may change prior to final publication. Citation information: DOI 10.1109/TPEL.2015.2403618, IEEE Transactions on Power Electronics

D. Luminous Flux ϕ_v

According to the PET theory [21], the total luminous flux ϕ_v of the lighting system can be formulated as an asymmetric convex parabolic curve: $\phi_v = \alpha_1 P_d - \alpha_2 P_d^2 - \alpha_3 P_d^3$, where α_1, α_2 and α_3 are positive coefficients and P_d is the LED power. Since the operating range normally lies on the left hand side of the peak of this parabolic curve and α_3 is usually much smaller than the other two coefficients, the term $\alpha_3 P_d^3$ (which primarily affects the part of the curve on the right-hand side of the peak where P_d is large) can be neglected. The total luminous flux of N LED devices with ambient temperature of T_a can be expressed as:

$$\phi_v = NE_o \left\{ \left[1 + k_e \left(T_a - T_o \right) \right] P_d + k_e k_h \left(R_{jc} + NR_{hs} \right) P_d^2 \right\} \tag{6}$$

As shown in Fig 3, the measured k_e is negative for OLED device, so (6) fits into the form of $\phi_v = \alpha_1 P_d - \alpha_2 P_d^2$. The PET theory points to an important issue in this luminous flux equation that increasing the LED power will not always increase the luminous flux output. The luminous flux increases with increasing LED power up to a maximum value. Beyond the maximum flux operating point, further increase in the LED power will lead to luminous flux drop.

The experimental power range for Lumiotec OLED is from 0.5 W to 6.5 W and that for Osram OLED is from 0.4 W to 4.6 W, with the ambient temperature set at 20 ^{o}C. The luminous flux are measured 20 minutes after driving the OLED. Based on the measured results for Fig. 3, Fig. 4 and Fig. 5, the parameters required for the PET modeling for the OLED samples can be obtained. For Lumiotec OLED (model number: P06A0203N-A13A), k_h=0.905 to 0.937 (T_j is from 25.2 ^{o}C to 128.9 ^{o}C), k_e=-0.00071, E_0=25.8 lm/W, R_{jc}=0.59 ^{o}C/W, T_0=25 ^{o}C, T_a=20 ^{o}C and N=1. For Osram

This article has been accepted for publication in a future issue of this journal, but has not been fully edited. Content may change prior to final publication. Citation information: DOI 10.1109/TPEL.2015.2403618, IEEE Transactions on Power Electronics

OLED (model number: OSP1F00WW303c1000), k_h=0.959 to 0.987 (T_j is from 28.8 ^{o}C to 133.1 ^{o}C), k_e=-0.0019, E_0=14.8 lm/W, R_{jc}=3.1 ^{o}C/W, T_0=25 ^{o}C, T_a=20 ^{o}C and N=1. Putting these device parameters into (6), the theoretical luminous flux as a function of OLED power can be derived. The measured and calculated luminous flux-OLED power curves of the OLED devices mounted on their respective heatsinks with different heatsink temperatures are plotted in Fig. 6. The agreement between measured and calculated is reasonably good. The maximum relative error between measured and calculated results is 12.8%, the minimum relative error is about 1.2%, and the average relative error is about 4.2%.

It should be noted that the measured luminous flux for Lumiotec and Osram OLED device increases fairly linearly with P_d for a large range of electrical power, because their k_e and R_{jc}+R_{hs} (the convection thermal resistance is small due to large area of substrate) are very small when compared with those of inorganic LEDs. In particular, the low R_{jc} of the Lumiotec sample enables heat dissipation to be transferred out of the junction, thereby keeping k_e very low and minimizing the temperature sensitivity of the luminous efficacy.

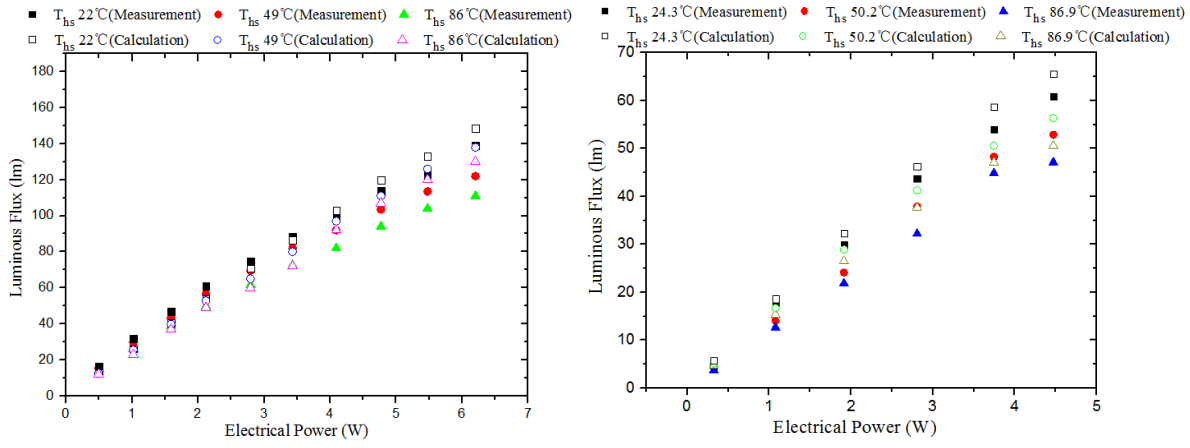

(a) (b)

Fig. 6 Measured and calculated luminous flux versus electrical power (a) Lumiotec LTS-10015 (b) Osram Orbeos CMW-031

This article has been accepted for publication in a future issue of this journal, but has not been fully edited. Content may change prior to final publication. Citation information: DOI 10.1109/TPEL.2015.2403618, IEEE Transactions on Power Electronics

Remarks:

Based on the above measured results for OLED devices, two important observations can be made:

(i) The relative low values of R_{jc} and k_e of OLEDs allow the flux-power relationship to be more linear than that of inorganic LEDs. This simplifies the dimming control and thermal design of OLED systems.

(ii) Due to the nonlinear flux-power curves of inorganic LEDs, PWM or Bi-level drive are needed to provide better linear control of the light intensity as compared to DC drive [35]. However, driving inorganic LEDs using PWM or Bi-level techniques introduces additional efficacy loss that is otherwise not present with DC driving methods. Such problems are not serious in the dimming control of OLEDs.

E. Spectral Power Distribution(SPD)

The chromatic aspects of OLEDs can be accounted for using spectral power distribution. The asymmetrical SPD of monochrome LED are typically modeled with a Gaussian function:

$$P_\lambda = P_{opt}\frac{1}{\sigma\sqrt{2\pi}}\exp[-0.5*\frac{(\lambda-\lambda_{peak})^2}{\sigma^2}] \tag{7}$$

where P_{opt} is the optical power of SPD, σ is dependent on the peak wavelength λ_{peak} and FWHM $\Delta\lambda$. FWHM is the full width at half maximum, which describes the spectral width of the emitting light.

$$\sigma = \frac{\lambda_{peak}^2\Delta E}{2hc\sqrt{2\ln 2}} = \frac{\lambda_{peak}^2\left(\frac{hc}{\lambda_1}-\frac{hc}{\lambda_2}\right)}{2hc\sqrt{2\ln 2}} = \frac{\lambda_{peak}^2\left(\frac{hc\Delta\lambda}{\lambda_1\lambda_2}\right)}{2hc\sqrt{2\ln 2}} \tag{8}$$

$$P_\lambda = \sum_{m=1}^{m=n} P_{\lambda,\mathrm{m}} \tag{9}$$

This article has been accepted for publication in a future issue of this journal, but has not been fully edited. Content may change prior to final publication. Citation information: DOI 10.1109/TPEL.2015.2403618, IEEE Transactions on Power Electronics

The SPD of a white LED using yellow YAG phosphor and blue LED chip can theoretically be predicted by a multi-SPD model [36]. With the help of such a multi-SPD model in (9), the reference SPD of an OLED can be constructed. Due to temperature effects on the peak wavelength λ_{peak} and FWHM $\Delta\lambda$, the peak wavelength and FWHM of multi-SPD can be expressed as

$$\lambda_{peak,\mathrm{m}}\left(T_j\right) = k_{peak,\mathrm{m}}\left(T_j - T_o\right) + \lambda_{peak,\mathrm{m,r}} \tag{10}$$

$$\Delta\lambda_m(T_j) = k_{\Delta\lambda,m}(T_j - T_0) + \Delta\lambda_{m,r} \tag{11}$$

where $\lambda_{peak,m}$, $k_{peak,m}$, $\lambda_{peak,m,r}$, $\Delta\lambda_m$, $k_{\Delta\lambda,m}$ and $\Delta\lambda_{m,r}$ are the peak wavelength, an coefficient for the temperature effect on the peak wavelength, the reference peak wavelength, the FWHM, a coefficient of the temperature effect on FWHM and the reference peak wavelength of the m^{th} SPD, respectively.

Due to the optical power variation caused by the injection current and temperature, the optical power $P_{opt,m}$ of m^{th} SPD can be expressed as:

$$P_{opt,m}(T_j, P_d) = (\alpha_m T_j + \beta_m)(\chi_m P_d + \gamma_m) \tag{12}$$

where α_m, β_m, χ_m and γ_m are the temperature and electrical power coefficients for the optical power of the m^{th} SPD.

The required parameters in (9)-(12) of Lumiotec and Osram OLED samples can be obtained from their measured light spectra. For each OLED sample, the number of SPDs can be determined from the number of peaks in the spectrum. Fig. 7(a) shows the measured spectrum of the Lumiotec sample. It can be seen that there are 4 peaks. Therefore, this spectrum can be considered as the summation of four SPDs. The spectrum of the Osram sample is shown in Fig. 7(b). It consists of 3 peaks and so can be modeled as the summation of 3 SPDs. Based on this methodology, the parameters of the spectra of the two OLED samples are obtained numerically based on the measured spectra and shown in Table IV and V, respectively. The calculated SPDs are displayed

This article has been accepted for publication in a future issue of this journal, but has not been fully edited. Content may change prior to final publication. Citation information: DOI 10.1109/TPEL.2015.2403618, IEEE Transactions on Power Electronics

with their measured counterparts in Fig. 7.

For the Lumiotec OLED, the SPDs of the Red and Green colors are for their respective phosphorescent materials and those of the Blue color (double peaks) are for the phosphorescent or fluorescent materials. As shown in Table IV, the peak wavelength and FWHM of the green phosphorescent materials (3rd SPD) have more temperature shift ($k_{peak,3}$=-0.05228, $k_{\Delta\lambda,3}$=0.0377) than those of the blue and red SPDs. For the Osram OLED, the SPDs of the red and green colors are based on phosphorescent materials. The blue color is likely due to fluorescent material. Table V shows that the peak wavelength and FWHM of red phosphorescent materials (3rd SPD) have more temperature shift ($k_{peak,3}$=-0.067, $k_{\Delta\lambda,3}$=0.104) than those of the blue and green colors. The measured and calculated values of the CCT (Correlated Color Temperature) of the two OLED samples are included in Fig. 8. It is noted that the calculated results are generally consistent with practical measurements. The absolute error is less than 100K. Their good agreement confirms the accuracy of the multi-SPD modeling method for OLED color characteristics.

Table IV The required parameters for multi-SPD model of Lumiotec LTS-10015

	m=1(blue)	m=2(blue)	m=3(green)	m=4(red)
$k_{peak,m}$ (nm/ ^{o}C)	-0.01551	-0.00218	-0.05228	-0.00878
$\lambda_{peak,m,r}$ (nm)	474.8	450.5	525.6	616.2
$k_{\Delta\lambda,m}$ (nm/ ^{o}C)	-0.03346	0.0297	0.0377	0.08373
$\Delta\lambda_{m,r}$ (nm)	23.4	17.6	47.6	75.9
α_m	-0.0081	-0.00364	-0.00173	-0.00297
β_m	1.21	1.11	1.04	1.08
χ_m	0.0072	0.0098	0.0217	0.0357
γ_m	0.00002	0.0006	0.0048	0.0061

This article has been accepted for publication in a future issue of this journal, but has not been fully edited. Content may change prior to final publication. Citation information: DOI 10.1109/TPEL.2015.2403618, IEEE Transactions on Power Electronics

Table V The required parameters for multi-SPD model of Osram Orbeos CMW-031

	m=1(blue)	m=2(green)	m=3(red)
$k_{peak,m}$ (nm/ °C)	-0.0127	-0.0505	-0.067
$\lambda_{peak,m,r}$ (nm)	470.2	511.3	609.9
$k_{\Delta\lambda,m}$ (nm/ °C)	0.0407	0.0415	0.104
$\Delta\lambda_{m,r}$ (nm)	28.1	34.3	82.7
α_m	0.0019	-0.00269	-0.00669
β_m	0.934	0.0010	1.168
χ_m	0.00352	0.0052	0.0272
γ_m	0.0011	0.0014	0.0046

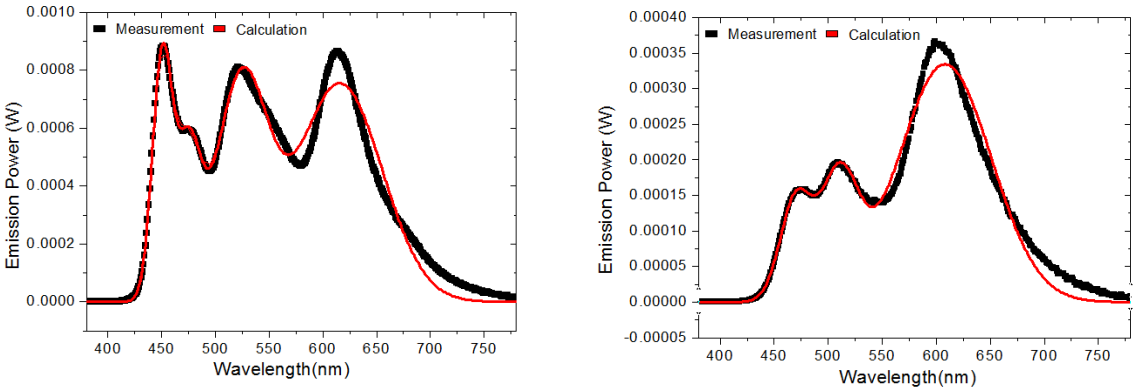

(a) (b)

Fig. 7 Measured and calculated spectral power distribution at current of 0.3A (a) Lumiotec LTS-10015 (b) Osram Orbeos CMW-031

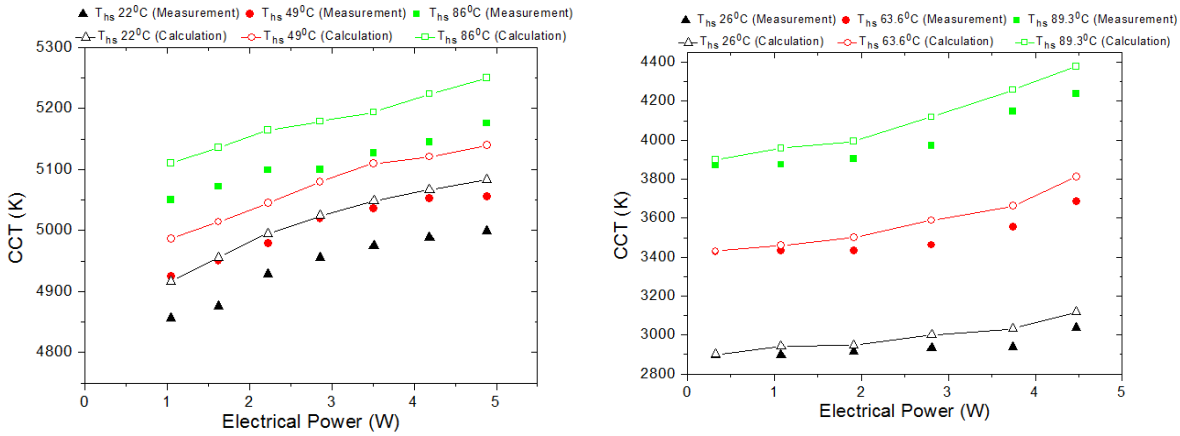

(a) (b)

Fig. 8 Measured and calculated CCT with temperature and electrical power (a) Lumiotec LTS-10015 (b) Osram Orbeos CMW-031

This article has been accepted for publication in a future issue of this journal, but has not been fully edited. Content may change prior to final publication. Citation information: DOI 10.1109/TPEL.2015.2403618, IEEE Transactions on Power Electronics

F. Luminance Distribution and Uniformity

Unlike inorganic LEDs which have small surface areas and can be considered as point sources, OLEDs have relatively large surface areas for illumination. The resistivity of the transparent electrode could lead to considerably lateral voltage drop if the lateral current flow reaches a certain value. Luminance of the OLED depends on the voltage over the organic layers and may also become inhomogeneous. Therefore, the luminance distribution and uniformity of OLEDs deserve more attention. The conductivity of the electrode material and the size of the pixel play an important role in this inhomogeneity [37]. Assuming that the p-type metal contact has equal potential and that the voltage across the vertical series resistance is much larger than *kT/e*, the current distribution can be expressed as [38]

$$J(x) = J(0)\exp\left(-\frac{x}{D_s}\right) \tag{13}$$

where *J(0)* is the current density at the p-type mesa edge, *x* is distance from p-type mesa edge and D_s is defined as the current spreading length.

$$D_s = \sqrt{\frac{(p_c + p_p t_p) t_n}{p_n}} \tag{14}$$

where p_c is the specific p-type contact resistance; p_p/p_n and t_p/t_n are electrical resistivity and thickness of the p/n type layers, respectively.

Luminance can be expressed as

$$L(x) = E_J J(x) = E_J J(0)\exp\left(-\frac{x}{D_s}\right) \tag{15}$$

where E_J is the efficiency coefficient relating the current density to luminance.

Luminance uniformity *U* can be defined as

This article has been accepted for publication in a future issue of this journal, but has not been fully edited. Content may change prior to final publication. Citation information: DOI 10.1109/TPEL.2015.2403618, IEEE Transactions on Power Electronics

$$U = 1 - \frac{L_{ave} - L_{\min}}{L_{ave}} \tag{16}$$

where L_{ave} is the average luminance, L_{min} is the minimum luminance, U is the luminance uniformity. If U is close to 1, the luminance distribution achieves perfect homogeneity.

According to the measured results of the luminance distribution with different injection current levels, the current spreading length D_s could be extracted based on the (15), as shown in Fig 11. It is found that the variation D_s with the injection current exhibits a parabolic distribution. Therefore, it can be expressed as

$$D_s = aI^2 + bI + c \tag{17}$$

where a, b and c can be extracted by a curve-fitting method based on the measured results in Fig. 12.

In order to estimate the luminance uniformity, (15) can be rewritten as

$$L(x) \approx E_J J(0)\left(1 - \frac{x}{D_s} + \frac{x^2}{D_s^2}\right) \tag{18}$$

Putting (17) into (18), the luminance distribution can be rewritten as

$$L(x) \approx E_I I(0)\left(1 - \frac{x}{aI^2 + bI + c} + \frac{x^2}{\left(aI^2 + bI + c\right)^2}\right) \tag{19}$$

where E_I is efficiency coefficient relating current to luminance. For a given injection current I, the minimum luminance is:

$$\begin{cases} L_{\min} \approx E_I I(0) \text{ if } D \geq D_s \\ L_{\min} \approx E_I I(0)\exp\left(\dfrac{D}{D_s}\right) \text{ if } D < D_s \end{cases} \tag{20}$$

The average luminance can be given as

This article has been accepted for publication in a future issue of this journal, but has not been fully edited. Content may change prior to final publication. Citation information: DOI 10.1109/TPEL.2015.2403618, IEEE Transactions on Power Electronics

$$L_{ave} = \frac{\sum_{m=1}^{n} L_I \exp\left(\frac{\frac{mD}{n}}{aI^2 + bI + c} \right)}{n} \tag{21}$$

where n is division number across the target length D, L_I is the initial luminance across the target length D.

Putting (20) and (21) into (16), the luminance uniformity can be expressed as

$$U = 1 - \frac{L_{ave} - L_{\min}}{L_{ave}} = \begin{cases} 1 - \dfrac{\sum_{m=1}^{n} L_I \exp\left(\dfrac{mD}{n\left(aI^2 + bI + c\right)} \right) - nL_I}{\sum_{m=1}^{n} L_I \exp\left(\dfrac{mD}{n\left(aI^2 + bI + c\right)} \right)} & \text{if } D \geq D_s \\ 1 - \dfrac{\sum_{m=1}^{n} L_I \exp\left(\dfrac{mD}{n\left(aI^2 + bI + c\right)} \right) - nL_I \exp\left(\dfrac{D}{D_s} \right)}{\sum_{m=1}^{n} L_I \exp\left(\dfrac{mD}{n\left(aI^2 + bI + c\right)} \right)} & \text{if } D < D_s \end{cases} \tag{22}$$

Several observations can be drawn from the above results.

(i) The current spreading length is related to the injection current. For a given current, the minimum luminance can be determined by (17). The current spreading length has a minimum value because a in (17) is a positive coefficient based on practical measurements.

(ii) The accuracy of the average luminance depends on n. A high value of n improves the resolution and accuracy of average luminance.

(iii) The luminance uniformity is related to the injection current, n (i.e. resolution) and target length D. If the target D is larger than current spreading length D_s, the minimum luminance is located at D_s. If the target D is lower than current spreading length D_s, the minimum luminance is located at D.

The measured luminance distributions across the two OLED samples at a current of 0.3 A are

This article has been accepted for publication in a future issue of this journal, but has not been fully edited. Content may change prior to final publication. Citation information: DOI 10.1109/TPEL.2015.2403618, IEEE Transactions on Power Electronics

included in Fig. 9. The electrical power for Lumiotec OLED is from 0.56 W (current for 0.1 A) to 4.08 W (current for 0.6 A).The electrical power for Osram OLED is from 0.32 W (current for 0.1 A) to 2.22 W (current for 0.6 A). The position of OLED samples without heatsink is vertical, while the ambient temperature of 20 ^{o}C. It can be seen that the luminous distributions are not uniform. In both cases, the luminance in the central regions is the lowest. It should however be noted that such nonuniform distribution is not caused by uneven thermal distribution. The measured surface temperature distribution across the two OLED samples at a current of 0.3 A are displayed in Fig. 10. The emissivity of Lumiotec and Osram OLEDs is 0.7 and 0.85 respectively when the measurements are made. The temperature distributions in both cases are fairly uniform. The maximum discrepancy in Fig. 10(a) and (b) are 1.1 ^{o}C and 2.9 ^{o}C, respectively. It is noted that the maximum temperature points do not appear in the centers. This important observation indicates that it is the current spreading characteristics that cause the luminance inhomogeneity. The thermal distribution has minor effect on luminance distribution.

The luminance distribution of the Lumiotec and Osram samples are shown in Fig. 11. The luminance intensities of the two samples increase with the injection current, but the luminance uniformity deteriorates with increasing current. At low luminance intensity, luminance non-uniformity for the two samples is not obvious. However, at high luminance intensity, a steep increase of luminance non-uniformity occurs in both samples. At high luminance intensity, the luminance non-uniformity of the Osram sample is a slightly higher that of the Lumiotec sample. Using (15) and the measured luminance distribution in Fig. 11, the current spreading length can be extracted, as shown in Fig. 12. The required parameters in (22) are shown in Table VI. Putting these parameters into (22), the luminance uniformity can be calculated and compared with the measured results. As shown in Fig. 13, the experimental results have a good agreement with theoretical ones.

This article has been accepted for publication in a future issue of this journal, but has not been fully edited. Content may change prior to final publication. Citation information: DOI 10.1109/TPEL.2015.2403618, IEEE Transactions on Power Electronics

The Lumiotec sample has better luminous uniformity than the Osram sample. It is found that a larger current spreading length will lead to a better luminous uniformity.

Table VI Device parameters for used in (22)

	Lumiotec sample	Osram sample
n	30	30
D(mm)	30	35
a	1252.7	114.7
b	-1354.5	-1173.3
c	459.2	386.7

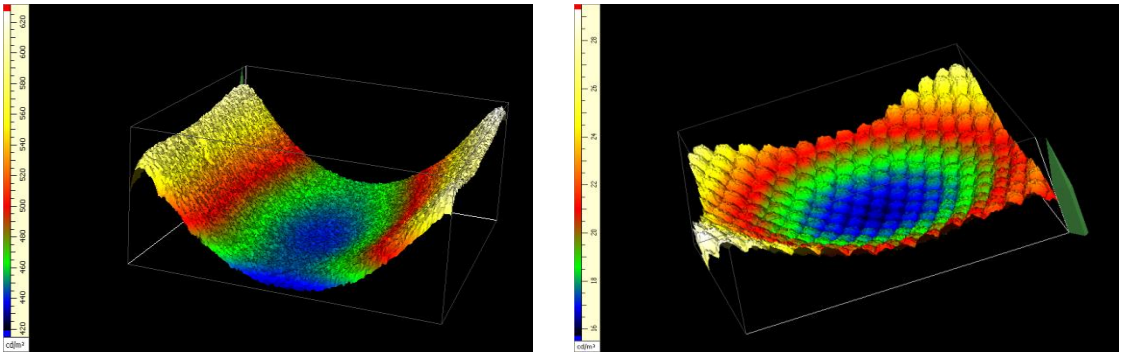

(a) (b)

Fig. 9 Measured 3D luminance profile at a current of 0.3A (a) Lumiotec LTS-10015 (b) Osram Orbeos CMW-031

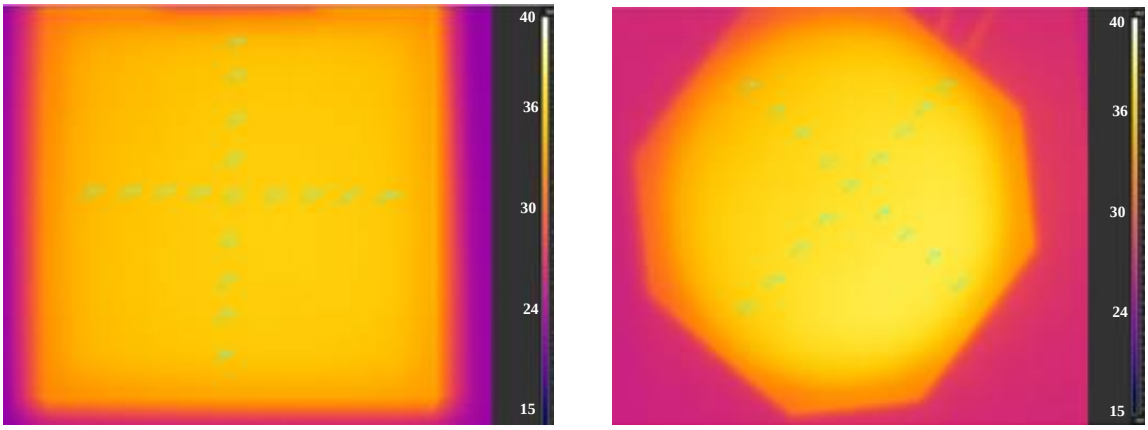

(a) (b)

Fig. 10 Measured temperature distribution at a current of 0.3A (a) Lumiotec LTS-10015 (b) Osram Orbeos CMW-031

This article has been accepted for publication in a future issue of this journal, but has not been fully edited. Content may change prior to final publication. Citation information: DOI 10.1109/TPEL.2015.2403618, IEEE Transactions on Power Electronics

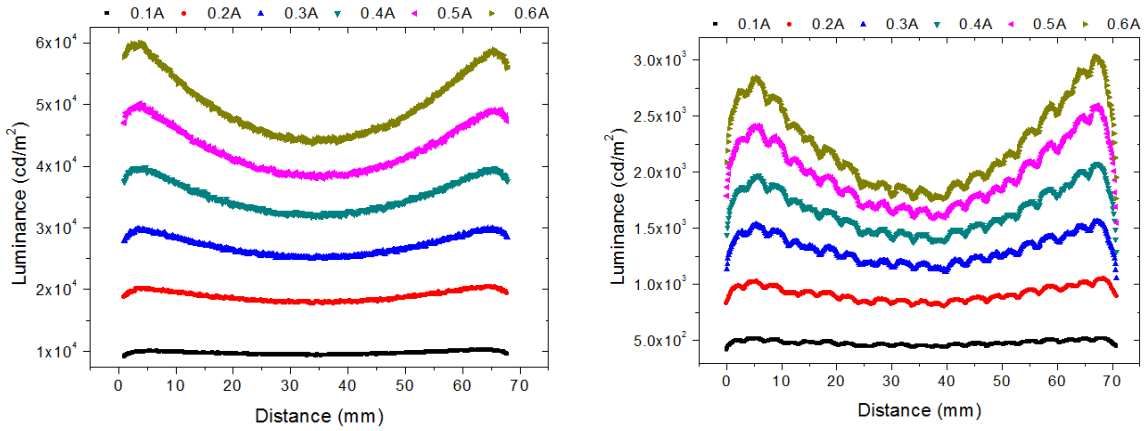

(a) (b)

Fig. 11 Measured luminance distribution at different current (a) Lumiotec LTS-10015 (b) Osram Orbeos CMW-031

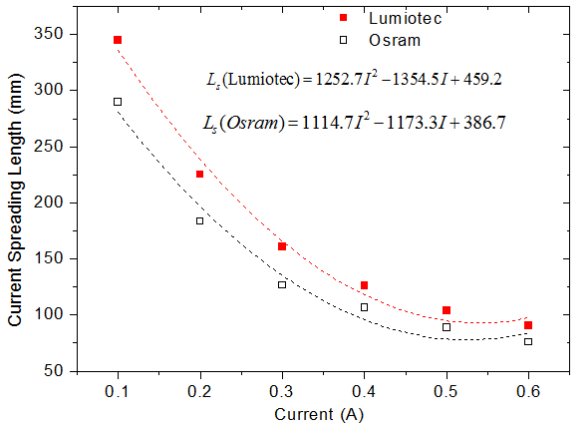

Fig. 12 Calculated current spreading length of Lumiotec and Osram OLED at different current

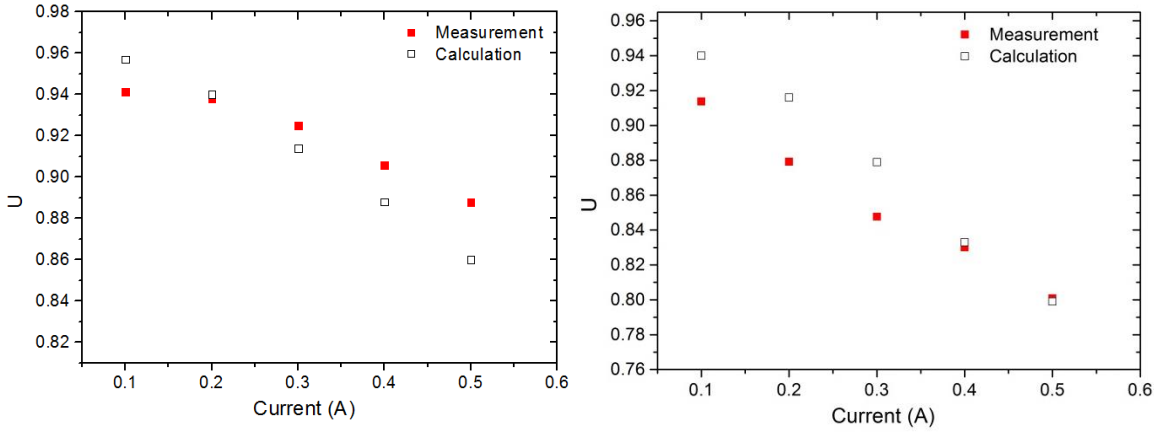

(a) (b)

Fig. 13 Measured and calculated luminance uniformity of OLEDs at different current (a) Lumiotec OLED (b) Osram OLED

This article has been accepted for publication in a future issue of this journal, but has not been fully edited. Content may change prior to final publication. Citation information: DOI 10.1109/TPEL.2015.2403618, IEEE Transactions on Power Electronics

IV. CONCLUSIONS

It is demonstrated in this paper that OLEDs with different structures can be characterized, modeled and analyzed with the combined use of the photo-electro-thermal theory and spectral power distributions. Such approach covers the photometric, electric, thermal and chromatic aspects of the OLEDs. Based on such a framework, the parameters of OLEDs can be determined and compared with those of inorganic LEDs. With large surface areas, OLEDs differ from inorganic LEDs in having a much lower thermal resistance and temperature sensitivity. Their luminous flux curves are relatively more linear than those of inorganic LEDs, making it easy to implement dimming control. Although OLEDs have generally higher heat dissipation coefficients than inorganic LEDs, such disadvantage is compensated by their large surface and contact areas which act as effective heat transfer paths.

For OLEDs, the materials of the substrates could affect their thermal performance significantly. Substrate with good thermal conductivity will lead to a low thermal resistance. However, it is discovered that uneven heat distribution over the surface of an OLED is not the main reason for the non-uniform luminance distribution. The main factor affecting the luminance uniformity is the current distribution which can be measured by the current spreading length. A larger the current spreading length is, the better the luminance uniformity becomes. The theoretical predictions of the OLEDs have been confirmed with experimental ones. Their good agreements confirm the validity of the combined used of the PET theory and SPD for studying OLED systems.

Acknowledgement:

This work is supported by the Hong Kong Research Grant Council (RGC) under the

Theme-based Research Project: T22-715/12 N. Choy would like to acknowledge the financial support of Chinese Academy of Sciences (CAS)-Croucher Funding Scheme for Joint Laboratories and the RGC Collaborative Research Fund (grant C7045-14E)

Reference

[1] Y. Kijima, N. Asai, N. Kishii, and S.Tamura, "RGB Luminescent from Passive-Matrix Organic LED's," *IEEE Trans. Electron. Devices.*, vol. 44, no. 8, pp.1222-1228, Aug. 1997.
[2] P. E. Burrows, G. Gu, V. Bulovic, Z. Shen, S. R. Forrest, and M. E. Thompson, "Achieving Full-Color Organic Light-Emitting Devices for Lightweight, Flat Panel Displays, " *IEEE Trans. Electron. Devices.*, vol. 44, pp.1188–1203, Aug. 1997.
[3] C.W. Tang and S. A. VanSlyke, "Organic electroluminescent diodes,"*Appl. Phys. Lett*., vol. 51, no. 12, pp. 913–915, Sep.1987.
[4] Y. G. Ma, H. Y. Zhang, J. C. Shen, C. M. Che, "Electroluminescence from triplet metal-ligand charge-transfer excited state of transition metal complexes," *Synthetic.Metals*., vol. 94, no. 3 pp.245–248, May. 1998.
[5] M. A. Baldo, D. F. Obrien, Y, You, A. Shoustikov, S. Sibley, M. E. Thompson, and S. R. Forrest, "Highly efficient phosphorescent emission from organic electroluminescent devices," *Nature*, vol. 395, pp. 151–154, Sep. 1998.
[6] W. C. H. Choy, W. K. Chan, Y. Yuan, "Recent advances in transition metal complexes and light-management engineering in organic optoelectronic devices," *Adv. M*at., vol. 26, no. 31, pp.5368–5399, Aug. 2014.
[7] H.H. Fong, W.C.H. Choy, K.N. Hui, and Y.J. Liang, "Organic light-emitting diodes based on a co-host electron transporting composite," *Appl. Phys. Lett*, vol. 88, no. 11, p.113510–113512, Mar. 2006.
[8] T. Zheng, and W.C.H. Choy, "High efficiency blue organic LEDs achieved by an integrated fluorescence-interlayer-phosphorescence emission architecture", *Adv. Function. Mater*., vol. 20, no. 4, pp.648–655, Feb. 2010.
[9] J. Kido, M. Kimura, and K. Nagai, "Multilayer white light-emitting organic electroluminescent device," *Science*, vol. 267, no. 5202, pp. 1332–1334, Mar.1995.
[10] B. D'Andrade, R. Holmes, and S. Forrest, "Efficient organic electrophosphorescent white light-emitting device with a triple doped emissive layer," *Adv. Mater*., vol. 16, no. 7, pp. 624–628, Apr. 2004.
[11] Y. Sun, N. C. Giebink, H. Kanno, B. Ma, M. E. Thompson, and S. R. Forrest, "Management of singlet and triplet excitons for efficient white organic light-emitting devices," *Nature*, vol. 440, pp. 908–912, Apr. 2006.
[12] S. W. Wen, M. T. Lee, and C. H. Chen, "Recent development of blue fluorescent OLED materials and devices," *J. Display Technol*., vol.1, no. 1, pp. 90–99, Sep. 2005.
[13] T.H. Zheng, and W.C.H. Choy, "High-efficiency blue fluorescent organic light emitting devices based on double emission layers," *J. Phys. D. Appl. Phys.*, vol. 41, no. 5, p.055103-1–055103-5, Jan. 2008.

[14] S. Reineke, F. Lindner, G. Schwartz, N. Seidler, K. Walzer, B. Lussem, and K. Leo, "White organic light-emitting diodes with fluorescent tube efficiency," *Nature*, vol. 459, pp. 234–238, Mar. 2009.
[15] Y. L. Chang, Y. Song, Z. Wang, M. G. Helander, J. Qiu, L. Chai, Z. Liu, G. D. Scholes, and Z. Lu "Highly efficient warm white organic light-emitting diodes by triplet exciton conversion," *Adv. Function. Mater.*, vol. 23, no. 6, pp. 705–712, Feb. 2013.
[16] G. Li, T. Fleetham, and J. Li, "Efficient and stable white organic light‐emitting diodes employing a single emitter, *Advanced Materials*, vol. 26, no. 18, pp. 2931-2936, May. 2014.
[17] S. Reineke, F. Lindner, G. Schwartz, N. Seidler, K. Walzer, B. Lussem, K. Leo "White organic light-emitting diodes with fluorescent tube efficiency," *Nature.*, vol. 459, pp. 234–238, Mar. 2009.
[18] J. Buytaert, J. Bleumers, A. Steen, and P. Hanselaer, "Optical determination of the junction temperature of OLEDs," *Org. Electron*, vol. 14, no. 11, pp. 2770-2776, Nov. 2013.
[19] Z. Kohári, E. Kollár, L. Pohl, and A. Poppe, "Nonlinear electro-thermal modeling and field-simulation of OLEDs for lighting applications II: luminosity and failure analysis," *Microelectr J*, vol. 44, no. 11, pp. 1011-1018, Nov. 2013.
[20] T. Nakayama, K. Hiyama, K. Furukawa, and H. Ohtani,"Development of phosphorescent white OLED with extremely high power efficiency and long lifetime," *SID Symp. Dig.*, vol.38, no.1,pp. 1018–1021, May. 2007.
[21] S. Y. R. Hui and Y. X. Qin, "A general photo-electro-thermal theory for light-emitting-diode (LED) systems," *IEEE Trans. Power. Electron.*, vol. 24, no. 8, pp.1967–1976, Aug. 2009.
[22] S. Y. R. Hui, H. T. Chen, and X. H. Tao, "An extended photoelectrothermal theory for LED systems - a tutorial from device characteristic to system design for general lighting [invited paper]," *IEEE Trans. Power. Electron.*, vol. 27, no. 1, pp.4571–4583, Nov. 2012.
[23] Lumiotec OLED Lighting Panels, Data Sheet P-06 http://www.lumiotec.eu/pdf/LTS-10015_P06_Spec_info_Eng.pdf
[24] Osram ORBEOS Mirrored OLED Round Lighting, Data Sheet CMW-031. Available: http://docs-europe.electrocomponents.com/webdocs/0f1a/0900766b80f1aee3.pdf
[25] G. Farkas, Q. V. V. Vader, A. Poppe, and G. Bognár, "Thermal investigation of high power optical devices by transient testing," *IEEE Trans. Compon. Pack. T.*, vol. 28, no. 1, pp: 45–50, Mar. 2005.
[26] E. F. Schubert, "Light-emitting diodes," *2nd ed. Cambridge, U. K: Cambridge Univ. Press*, 2006.
[27] Y. X. Qin, D. Y. Lin and S. Y. R. Hui, "A simple method for comparative study on the thermal performance of light emitting diodes (LED) and fluorescent lamps," *IEEE Trans. Power. Electron.*, vol. 24, no. 7, pp. 1811-1818, Jul. 2009.
[28] M. Furno, T. C. Rosenow, M. C. Gather, B. Lussem, and K. Leo, "Analysis of the external and internal quantum efficiency of multi-emitter, white organic light emitting diodes" *Appl. Phys. Lett.*, vol. 101, no. 14, pp. 143304-1–143304-4, Oct.2012.
[29] A. Cester, D. Bari, J. Framarin, N. Wrachien, G. Meneghesso, S. Xia, V. Adamovich, and J. J.Brown, "Thermal and electrical stress effects of electrical and optical characteristics of Alq3/NPD OLED", *Microelectron Reliab*, vol. 50, no. 9-11， pp. 1866-1870, Nov. 2010.
[30] H. T. Chen, X. H. Tao, and S. Y. R. Hui, "Estimation of optical power and heat dissipation coefficient for the photo-electro-thermal theory for LED systems," *IEEE Trans. Power. Electron.*, vol. 27, no. 4, pp. 2176–2183, Apr. 2012.
[31] X. F. Qi, and S. R. Forrest, "Thermal analysis of high intensity organic light-emitting diodes based on a transmission matrix approach", *J. Appl. Phys*, vol. 110, no. 12, PP.124516-1-124516-11, Dec.2011.
[32] K. J. Bergemann, R. Krasny, and S. R. Forrest, "Thermal properties of organic light-emitting diodes," *Org. Electron*, vol. 13, no. 9, pp. 1565-1568, Sep. 2012.
[33] H. T. Chen, S. C. Tan, S. Y. R. Hui, "Analysis and modeling of high-power phosphor-coated white light-emitting diodes with large surface area", *IEEE Trans. Power. Electron.*, vol. 30, no. 6,

pp. 3334–3344, Jun. 2015.
[34] J. Hu, L.Yang, and M. W. Shin, "Mechanism and thermal effect of delamination in light emitting diode packages*," Microelectro. J*, vol.38, no.2, pp.157–163, Feb.2007.
[35] S. C. Tan, "General n-level driving approach for improving electrical-to-optical energy-conversion efficiency of fast-response saturable lighting devices," *IEEE Trans. Industral. Electron*., vol. 57, no. 4, pp. 1342-1353, Apr. 2010.
[36] H. T. Chen and S. Y. R. Hui, "Dynamic prediction of correlated color temperature and color rendering index of phosphor-coated white light-emitting diodes," *IEEE Trans. Ind. Electron.*, vol. 61, no. 2, pp. 784–797, Feb. 2014.
[37] K. Neyts, M. Marescaux, A. U. Nieto, A. Elschner, W. Lovenich, K. Fehse, Q. Huang, K. Walzer, and K. Leo, "Inhomogeneous luminance in organic light emitting diode related to electrode resistivity" *J. Appl. Phys.*, vol. 100, no. 11, pp.114513-1–114513-4, Dec. 2006.
[38] X. Guo and E. F. Schubert, "Efficiency of GaN/InGaN light-emitting diodes with interdigitated mesa geometry", *Appl. Phys. Lett*., vol. 79, no. 13, pp. 1936–1938, Aug. 2001.